



Title	Multifractality of complex networks
Author(s)	Furuya, Shuhei; Yakubo, Kousuke
Citation	Physical Review E, 84(3), 036118 https://doi.org/10.1103/PhysRevE.84.036118
Issue Date	2011-09
Doc URL	http://hdl.handle.net/2115/47471
Rights	©2011 American Physical Society
Type	article
File Information	PRE84-3_036118.pdf



[Instructions for use](#)

Multifractality of complex networks

Shuhei Furuya^{*}

Department of Mathematical Informatics, The University of Tokyo, Tokyo 113-8656, Japan

Kousuke Yakubo[†]

Department of Applied Physics, Hokkaido University, Sapporo 060-8628, Japan

(Received 13 May 2011; published 30 September 2011)

We demonstrate analytically and numerically the possibility that the fractal property of a scale-free network cannot be characterized by a unique fractal dimension and the network takes a multifractal structure. It is found that the mass exponents $\tau(q)$ for several deterministic, stochastic, and real-world fractal scale-free networks are nonlinear functions of q , which implies that structural measures of these networks obey the multifractal scaling. In addition, we give a general expression of $\tau(q)$ for some class of fractal scale-free networks by a mean-field approximation. The multifractal property of network structures is a consequence of large fluctuations of local node density in scale-free networks.

DOI: 10.1103/PhysRevE.84.036118

PACS number(s): 89.75.Hc, 89.75.Fb, 64.60.al

I. INTRODUCTION

Inspired by the pioneering work by Song *et al.* [1], the fractal property of complex networks has been extensively studied recently [2–10]. The fractal property of a network is measured by the box-covering method in which the minimum number of subgraphs (boxes) of diameter l (in the sense of network distance) required to cover the fractal network is proportional to l^{-D_f} with the fractal dimension D_f . Most of real-world fractal networks are inhomogeneous in the sense of the scale-free property defined by a power-law degree distribution $P(k) \propto k^{-\gamma}$, where k is the number of connections of a node (degree) [11]. Thus, the number of nodes in a subgraph of size l depends strongly on whether the subgraph includes hubs and their neighboring nodes or not, which implies that the distribution of local node density is highly inhomogeneous. An inhomogeneous distribution of a physical quantity on a fractal object often exhibits the multifractal property [12–15]. In many of fractal objects embedded in Euclidean space, however, the underlying structure seldom shows the multifractal nature because of an exponentially thin tail of the mass distribution. On the contrary, we expect the multifractal scaling in a scale-free network due to large fluctuations of local node density. In this paper, we show analytically and numerically that fractal scale-free networks (FSFNs) can have the multifractal property in their structural features.

II. MULTIFRACTAL ANALYSIS OF NETWORKS

In order to explicate the possibility that a FSFN takes a multifractal structure, let us consider, at first, why conventional fractal structures do not possess the multifractal property. In the multifractal analysis, the behavior of a coarse-grained physical quantity on a fractal object is argued. Let x_i and μ_i be a physical quantity on the discretized position i and its normalized value

(measure), that is,

$$\mu_i = \frac{x_i}{\sum_j x_j}. \quad (1)$$

The coarse-grained measure (box measure) $\mu_{b(l)}$ is then given by $\mu_{b(l)} = \sum_{i \in b(l)} \mu_i$, where $b(l)$ is a box of size l in the system. If the spatial distribution of the physical quantity x does not bring a characteristic length scale, the q th moment of the box measure

$$\langle \mu_l^q \rangle = \sum_{b(l)} \mu_{b(l)}^q \quad (2)$$

has a power-law l dependence, namely, $\langle \mu_l^q \rangle \propto l^{\tau(q)}$, where the summation in Eq. (2) is taken over boxes of size l required to cover minimally the entire system. In the case that the exponent $\tau(q)$ (called as the mass exponent) is a nonlinear (linear) function of q , the distribution of the measure is regarded to be multifractal (unifractal). Here, we consider a constant mass of the site i as a physical quantity x_i . The normalized measure μ_i representing the mass density becomes constant and the box measure $\langle \mu_{b(l)} \rangle$ averaged over boxes is proportional to l^{D_f} , where D_f is the fractal dimension of the system. If the fluctuation of $\mu_{b(l)}$ over boxes is sufficiently small, Eq. (2) is approximated as

$$\langle \mu_l^q \rangle \sim \sum_{b(l)} \langle \mu_{b(l)} \rangle^q \sim l^{D_f(q-1)}. \quad (3)$$

Therefore we have the linear relation $\tau(q) = D_f(q-1)$ representing the unifractal nature of the mass density distribution. In fact, a narrow distribution of the box measure is widely observed in many fractals embedded in Euclidean space [16–20]. Thus, most of fractal systems take unifractal structures, with some exceptions such as mathematical multifractal sets as the two-scale Cantor set [21] and geochemical distribution of minerals [22–24]. The box measure $\mu_{b(l)}$ of node density in a FSFN, however, has large fluctuations over boxes [10]. This is because $\mu_{b(l)}$ of a box including a hub node can be much larger than that of a box without hubs. If the probability distribution function of the box measure has a fat tail like a power-law or log-normal form, $\mu_{b(l)}$ cannot be approximated

*sfuruya@stat.t.u-tokyo.ac.jp

†yakubo@eng.hokudai.ac.jp

by $\langle \mu_{b(l)} \rangle$ and the failure of Eq. (3) gives a possibility of the multifractal scaling in structures of complex networks.

When applying the multifractal analysis to complex networks, it is unavoidable that covering boxes (subgraphs) of network diameter l overlap each other [5], if every box includes the maximum number of nodes unless the subgraph diameter does not exceed l as in the conventional multifractal analysis [12]. Therefore, the measure μ_i defined by Eq. (1) cannot be normalized as $\sum_{b(l)} \mu_{b(l)} = 1$, and the mass exponent does not satisfy the basic condition $\tau(1) = 0$. In order to overcome this difficulty, we modify the definition of the measure as

$$\mu_i = \frac{x_i}{\sum_{b(l)} \sum_{j \in b(l)} x_j}. \quad (4)$$

In this definition, the normalization constant, and then μ_i , varies with the box size l . It is easy to confirm that the mass exponent calculated from Eq. (4) satisfies the general conditions $\tau(0) = -D_f$ and $\tau(1) = 0$ and for a unifractal system $\tau(q) = D_f(q - 1)$. We set hereafter $x_i = 1$ to analyze the multifractal nature of the node density in a complex network.

III. MULTIFRACTALITY OF (u,v) FLOWERS

Using the above definition of μ_i , we first examine analytically the multifractal property of the (u,v) -flower model [9]. This deterministic model provides a class of FSFNs. In this model, we start with the cycle graph consisting of $w \equiv u + v$ ($1 < u \leq v$) nodes and edges (the first generation). The network in the n th generation is obtained by replacing each edge in the $(n-1)$ th generation network by two parallel paths of u and v edges. The network with large n has the scale-free property with the degree exponent $\gamma = 1 + \log w / \log 2$ [9]. The number of nodes in the n th generation network is given by

$$v_n = \left(\frac{w-2}{w-1} \right) w^n + \left(\frac{w}{w-1} \right), \quad (5)$$

and the number of edges is w^n . In addition, when w is even, the diameter is written as

$$L_n = \left(\frac{u+v}{2} + \frac{v-u}{u-1} \right) u^{n-1} - \frac{v-u}{u-1}. \quad (6)$$

From the network formation algorithm, the n th generation network is constructed by w^{n-m} of (u,v) flowers in the m th generation, where $m < n$. This implies that if we cover the n th generation network by the m th generation subgraphs as shown in Fig. 1(a) the number of covering boxes $N_{b(L_m)}$ is w^{n-m} . Using Eq. (6), we can rewrite this relation as $N_{b(L_m)} = w^m [(L_m + b)/a]^{-\log w / \log u}$, where $a = (w/2 + b)/u$ and $b = (v-u)/(u-1)$. If the length L_m is large enough, we have the fractal dimension given by $D_f = \log w / \log u$ [9]. The above covering scheme (named as the covering scheme I), however, does not lead the minimum value of $N_{b(L_m)}$ for a fixed L_m . Let us consider the following covering scheme (named as the covering scheme II). At first, we cover the (u,v) flower by subgraphs of size L_m centered at the largest hubs, then the remaining network is covered by subgraphs centered at the second largest hubs. Repeating this procedure until all nodes are covered by subgraphs [as shown in Fig. 1(b)]

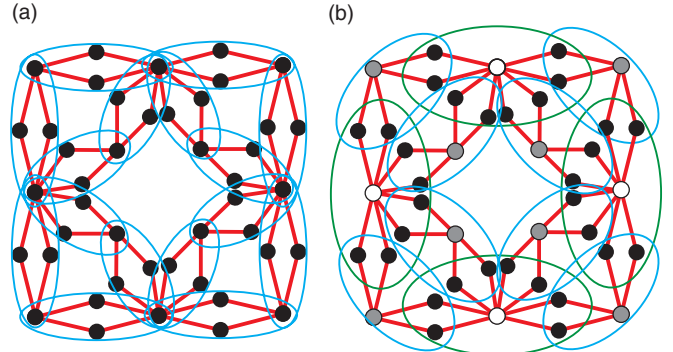


FIG. 1. (Color online) Two types of covering schemes for the (u,v) flower with $u = v = 2$ in the third generation. (a) The network is covered by 16 (u,v) flowers in the first generation (scheme I), and (b) the network is first covered by four subgraphs of size $l = 2$ centered at the largest hubs (white nodes) then covered by eight subgraphs centered at the second largest hubs (gray nodes) (scheme II).

number of covering boxes $N_{b(L_m)}$ becomes less than w^{n-m} . Although two covering schemes yield different $N_{b(L_m)}$, these are in proportion as shown later, and then the fractal dimension calculated by the covering scheme II is the same as that by scheme I. Therefore, both covering schemes are valid for the fractal analysis. In the *multifractal* analysis, however, we treat not only $N_{b(L_m)}$ ($= \langle \mu_{L_m}^{q=0} \rangle$) but also $\langle \mu_{L_m}^q \rangle$ for any q . Since the moment $\langle \mu_{L_m}^q \rangle$ calculated by the covering scheme I is generally not proportional to $\langle \mu_{L_m}^q \rangle$ by scheme II, we need to choose scheme II with less (probably minimum) covering boxes for the multifractal analysis of the (u,v) flower. It is, in general, quite important to cover a network by less number of boxes in the multifractal analysis comparing to the case of the fractal analysis.

Let us cover the (u,v) flower in the n th generation by boxes of size $l = L_m$ ($1 \ll m \ll n$) in the covering scheme II. The number of boxes $N_{b(s,L_m)}$ centered at the s th largest hubs is equal to the number of such hubs, thus we have

$$N_{b(s,L_m)} = v_s - v_{s-1} \quad (1 \leq s \leq n-m), \quad (7)$$

where $b(s,L_m)$ represents a box of size L_m centered at the s th largest hub and $v_0 = 0$. Since the number of nodes $\tilde{v}_s(L_m)$ in $b(s,L_m)$ is presented by

$$\tilde{v}_s(L_m) = 2^{n-m-s+1} (v_m/2 + 1) \simeq 2^{n-m-s} v_m, \quad (8)$$

the total number of nodes in all boxes, namely, the denominator of Eq. (4), is given by $\sum_{s=1}^{n-m} N_{b(s,L_m)} \tilde{v}_s(L_m)$. Using Eqs. (5), (7), and (8), the measure μ_i defined by Eq. (4) with $x_i = 1$ is thus expressed as

$$\mu_i = \frac{w-1}{w^n(w-2)}. \quad (9)$$

It should be noted that μ_i for the (u,v) flower is independent of the box size though the box measure given by Eq. (4) generally depends on l . Denoting μ_i independent of i by μ , the q th moment of the box measure is calculated from $\langle \mu_{L_m}^q \rangle = \sum_{b(s,L_m)} (\sum_{i \in b(s,L_m)} \mu)^q =$

$\sum_{s=1}^{n-m} N_{b(s,L_m)} [\mu \tilde{v}_s(L_m)]^q$. By means of Eqs. (5) and (7)–(9), the quantity $\langle \mu_{L_m}^q \rangle$ is calculated as

$$\begin{aligned} \langle \mu_{L_m}^q \rangle &= \frac{w^{n(1-q)}}{W_q} \left[\left(\frac{2^q}{w} \right)^{n-1} (W_q - 1) \left(\frac{L_m + b}{a} \right)^{\frac{q \log(w/2)}{\log u}} \right. \\ &\quad \left. + \left(\frac{L_m + b}{a} \right)^{\frac{(q-1) \log w}{\log u}} \right], \end{aligned} \quad (10)$$

where a and b are defined below Eq. (6), $W_q = (w - 2^q)/(w - 2)$, and the approximation $v_m \simeq w^m(w - 2)/(w - 1)$ is used. The dominant term in Eq. (10) for large L_m depends on q , and the mass exponent is given by

$$\tau(q) = \begin{cases} q \frac{\log(w/2)}{\log u} & \text{if } q \geq \frac{\log w}{\log 2}, \\ (q-1) \frac{\log w}{\log u} & \text{if } q < \frac{\log w}{\log 2}. \end{cases} \quad (11)$$

The nonlinear form of $\tau(q)$ indicates that local node densities of the (u,v) flower are distributed in a multifractal manner [25]. Although the above argument holds only for even values of w , we found that Eq. (11) is a good approximation also for odd w . It should be noted that $\langle \mu_{L_m}^q \rangle = w^{n(1-q)}[(L_m + b)/a]^{(q-1)\log w/\log u}$ obtained by scheme I is proportional to Eq. (10) for $q < \log w/\log 2$, but not otherwise.

It is generally difficult to find the way to cover minimally a given network because the minimization of the number of covering boxes is known to be NP hard. We then need to cover the network by a *less* number of boxes, as an approximation, in actual multifractal analyses. A variety of such covering methods have been proposed so far [1,3–8]. In order to clarify whether such covering techniques proven to be efficient for fractal analyses still work even in multifractal analyses sensitive to the covering way, we compare the analytical expression Eq. (11) with the numerically calculated $\tau(q)$ by adopting the compact-box-burning algorithm [4] modified to shorten the computing time [7]. The results shown in Fig. 2(a) clearly demonstrate the validity of this covering method.

IV. MEAN-FIELD ARGUMENT

Let us generalize our argument to some extent. We treat a FSFN of N nodes, whose degree distribution is given by $P(k) \propto k^{-\gamma}$. Covering the network minimally by $N_{b(l)}$ boxes of diameter l , the mean number of nodes $\langle v_l \rangle$ in a box is given by $N/N_{b(l)} \propto l^{-D_f}$. Regarding mutually connected boxes of size l as a renormalized network [1], the fractal property of the original network assures the relation $P_l(k_l) \propto k_l^{-\gamma}$, where $P_l(k_l)$ is the degree distribution function of the renormalized network. Here we assume that each renormalized node is statistically equivalent and the number of nodes $v_l(k_l)$ in a covering box corresponding to the renormalized node of degree k_l has negligibly small fluctuations over boxes. In this mean-field approach, the quantity $v_l(k_l)$ is represented by its mean value,

$$v_l(k_l) = \frac{k_l}{\langle k \rangle} \langle v_l \rangle, \quad (12)$$

where $\langle k \rangle = \langle k_l \rangle$ is the average degree of the original network. The (u,v) flower satisfies Eq. (12) rigorously in the thermodynamic limit ($n \rightarrow \infty$). Since the box measure $\mu_{b(l)}$ is given

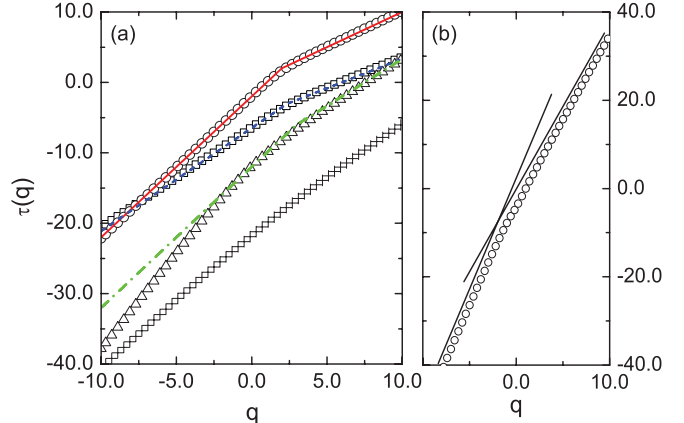


FIG. 2. (Color online) Mass exponent $\tau(q)$ for several fractal complex networks. (a) Solid line (red line) and circles indicate $\tau(q)$ for the (u,v) flower with $u = v = 2$ calculated by Eq. (11) and by the numerical box covering for the network in the eighth generation ($N = 43\,692$), respectively. Squares represent numerical results of $\tau(q)$ for the network formed by the minimal model with $m = 2$ in the seventh generation ($N = 15\,626$). Dashed line (blue line) indicates the theoretical curve for this minimal model predicted by Eq. (13). Triangles and crosses show $\tau(q)$ for the giant components of the fitness model ($N = 100\,000$) and the Erdős-Rényi random graph ($N = 200\,000$) at their percolation transitions, respectively. The degree exponent for the fitness model is set to be $\gamma = 4.0$. We averaged $\langle \mu_l^q \rangle$ over 100 realizations both for the fitness and the random graph models. Dashed-dotted line (green line) indicates $\tau(q)$ given by Eq. (13) with $\gamma = 4.0$ and $D_f = 2$ corresponding to the fitness model. Results except for the (u,v) flower are shifted vertically for clarity though all $\tau(q)$ actually pass through $\tau(1) = 0$. (b) The mass exponent $\tau(q)$ for the WWW is presented by circles. Straight lines indicating the slopes of $\tau(q)$ for $q \ll -1$ and $q \gg 1$ are just guides to the eye.

by $v_l(k_l)$ normalized by N , that is, $\mu_{b(l)} = k_l / [\langle k \rangle N_{b(l)}] \propto (k_l / \langle k \rangle) l^{D_f}$, the q th moment $\langle \mu_l^q \rangle$ can be calculated by Eq. (2). Considering that the maximum degree k_{\max} is proportional to $N^{1/(\gamma-1)}$, we have $\langle \mu_l^q \rangle \propto l^{(q-1)D_f}$ for $q < \gamma - 1$ and $\langle \mu_l^q \rangle \propto l^{qD_f(\gamma-2)/(\gamma-1)}$ for $q \geq \gamma - 1$. Therefore, the mass exponent $\tau(q)$ of this network is presented by

$$\tau(q) = \begin{cases} (q-1)D_f & \text{if } q < \gamma - 1 \\ qD_f \left(\frac{\gamma-2}{\gamma-1} \right) & \text{if } q \geq \gamma - 1. \end{cases} \quad (13)$$

This result implies that FSFNs satisfying Eq. (12) generally take multifractal (bifractal) structures. Our result Eq. (11) for the (u,v) flower is a special case of Eq. (13).

In order to confirm the validity of the above mean-field argument, we numerically calculate the mass exponent for the minimal model proposed by [2], employing the compact-box-burning algorithm [4]. A network formed by this model possesses the scale-free property with the degree exponent $\gamma = 1 + \log(2m+1)/\log m$ and takes a fractal structure with the fractal dimension $D_f = \log(2m+1)/\log 3$. The minimal model also satisfies Eq. (12) as in the case of the (u,v) -flower model [2]. The nonlinear behavior of numerically calculated $\tau(q)$ indicated by squares in Fig. 2(a) agrees quite well with the theoretical prediction Eq. (13). As an example of networks

not satisfying Eq. (12) due to large fluctuations of $v_l(k_l)$, we treat a stochastic model of FSFNs, namely the fitness model proposed by [26]. A network formed by this algorithm also has the scale-free property and the giant component exhibits the fractal nature at the percolation transition [7]. Triangles in Fig. 2(a) represent $\tau(q)$ for FSFNs formed by the fitness model with $\gamma = 4.0$ and $D_f = 2$ [7]. The exponent $\tau(q)$ is also a nonlinear function of q , which suggests the multifractal structure of the network, but cannot be described by Eq. (13). Finally, we calculate the mass exponent $\tau(q)$ for the World Wide Web (WWW) with 325 729 nodes [27], which is known to be a representative real-world FSFN [1]. Although the nonlinearity of $\tau(q)$ is weak as shown in Fig. 2(b) and the result is not described by Eq. (13), two tangential lines in the extreme regimes $q \ll -1$ and $q \gg 1$ have definitely different slopes, which shows the multifractal structure of the WWW. The multifractal property found in these networks is obviously caused by the scale-free nature of networks. In fact, $\tau(q)$ for the giant component of the Erdős-Rényi random graph [28] at the percolation threshold is, as shown by crosses in Fig. 2(a), a linear function of q , where the giant component is fractal but not scale free.

V. SUMMARY

In conclusion, we demonstrated analytically and numerically that fractal scale-free networks (FSFNs) can take multifractal structures in which the fractal dimension is not enough to characterize fractality of systems. The multifractal nature is caused by large fluctuations in local node density in scale-free networks. Although all examples treated in this paper exhibit the multifractal nature, further investigations are needed to clarify whether any FSFNs take multifractal structures. It is also crucial to study how the multifractal property affects physical phenomena or dynamics on complex networks.

ACKNOWLEDGMENTS

This work was supported by a Grant-in-Aid for Scientific Research (No. 22560058) and Grant-in-Aid for JSPS Fellows (No. 22-3380) from Japan Society for the Promotion of Science. Numerical calculations in this work were performed on the facilities of the Supercomputer Center, Institute for Solid State Physics, University of Tokyo. We are grateful to a referee for the crucial idea for the mean-field argument that improves the paper drastically.

-
- [1] C. Song, S. Havlin, and H. A. Makse, *Nature (London)* **433**, 392 (2005).
 - [2] C. Song, S. Havlin, and H. A. Makse, *Nat. Phys.* **2**, 275 (2006).
 - [3] K.-I. Goh, G. Salvi, B. Kahng, and D. Kim, *Phys. Rev. Lett.* **96**, 018701 (2006).
 - [4] C. Song, L. K. Gallos, S. Havlin, and H. A. Makse, *J. Stat. Mech.: Theory Exp.* (2007) P03006.
 - [5] J. S. Kim, K.-I. Goh, B. Kahng, and D. Kim, *Chaos* **17**, 026116 (2007).
 - [6] J. S. Kim, K.-I. Goh, G. Salvi, E. Oh, B. Kahng, and D. Kim, *Phys. Rev. E* **75**, 016110 (2007).
 - [7] F. Kawasaki and K. Yakubo, *Phys. Rev. E* **82**, 036113 (2010).
 - [8] L. Gao, Y. Hu, and Z. Di, *Phys. Rev. E* **78**, 046109 (2008).
 - [9] H. D. Rozenfeld, S. Havlin, and D. ben-Avraham, *New J. Phys.* **9**, 175 (2007).
 - [10] M. Mitobe and K. Yakubo, *J. Phys. Soc. Jpn.* **78**, 124002 (2009).
 - [11] A.-L. Barabási and R. Albert, *Science* **286**, 509 (1999).
 - [12] G. Paladin and A. Vulpiani, *Phys. Rep.* **156**, 147 (1987).
 - [13] H. E. Stanley and P. Meakin, *Nature (London)* **335**, 405 (1988).
 - [14] B. B. Mandelbrot, *J. Fluid Mech.* **62**, 331 (1974).
 - [15] T. A. Witten Jr. and L. M. Sander, *Phys. Rev. Lett.* **47**, 1400 (1981).
 - [16] S. T. Bramwell, P. C. W. Holdsworth, and J.-F. Pinton, *Nature (London)* **396**, 552 (1998).
 - [17] M. Mitobe and K. Yakubo, *J. Phys. Soc. Jpn.* **78**, 074006 (2009).
 - [18] B. Zheng, *Phys. Rev. E* **67**, 026114 (2003).
 - [19] K. Binder, *Z. Phys. B* **43**, 119 (1981).
 - [20] C. Federrath, J. Roman-Duval, R. S. Klessen, W. Schmidt, and M.-M. Mac Low, *Astron. Astrophys.* **512**, A81 (2010).
 - [21] T. Ficker, *Phys. Rev. A* **40**, 3444 (1989).
 - [22] M. A. Gonçalves, *Math. Geolog.* **33**, 41 (2001).
 - [23] F. Agterberg, *Math. Geolog.* **39**, 1 (2007).
 - [24] S. Xie, Q. Cheng, X. Xing, Z. Bao, and Z. Chen, *Geoderma* **160**, 36 (2010).
 - [25] The singularity exponent $\alpha = \partial \tau(q)/\partial q$ takes only two values for Eq. (11) while the exponent α varies continuously for usual multifractals. In this sense, the (u, v) flower might be regarded as a *bifractal* object.
 - [26] G. Caldarelli, A. Capocci, P. De Los Rios, and M. A. Muñoz, *Phys. Rev. Lett.* **89**, 258702 (2002).
 - [27] R. Albert, H. Jeong, and A.-L. Barabási, *Nature (London)* **401**, 130 (1999).
 - [28] P. Erdős and A. Rényi, *Publ. Math.* **6**, 290 (1959).